Applied Chemical Engineering (2021) Volume 4 Issue 2
doi:10.24294/ace.v4i2.1358

ORIGINAL RESEARCH ARTICLE

Synthesis of Pd/CeO_x/Nano-graphite composite cathode for electro-catalytic degradation of phenol

Yuhang Zhang[1,2], Yang Qu[1,2], Zhijun Li[1,2], Li Yu[1], Liqiang Jing[1,2*]

[1] *School of Chemistry and Materials Science, Heilongjiang University, Harbin 150080, China. E-mail: frog17@126.com; quyang@hlju.edu.cn*

[2] *Key Laboratory of Functional Inorganic Material Chemistry, Ministry of Education of the People's Republic of China, Harbin 150080, China. E-mail: jinglq@hlju.edu.cn*

ABSTRACT

To improve the cathode electro-catalytic degradation performance of electrochemical advanced oxidation processes (EAOP), Pd metal and CeO_x co-modified Nano-graphite (Pd/CeO_x/Nano-G) composite was synthesized by chemical precipitation and reduction methods, and Pd/CeO_x/Nano-G cathode was prepared by a hot-pressing method. The as-prepared composite and electrode were characterized by X-ray photoelectron spectroscopy, X-ray diffraction and scanning electrons microscopy. Results revealed that the mix-crystal structural CeOx (Ce_2O_3 and CeO_2) and Pd^0 metal were formed. The cathode was applied for the electro-catalytic degradation of phenol wastewater. The degradation efficiency of phenol by $Pd_{1.0}$/$CeO_{x5.0}$/Nano-G cathode reached 99.6% within 120 min degradation, which were higher than that of $CeO_{x5.0}$/Nano-G and Nano-G cathodes. Both of the Pd metal and CeO_x could improve the O_2 reduction to H_2O_2 and promote the H_2O_2 dissociation to •OH for phenol oxidation. Additionally, the effects of electro-catalytic reaction parameters on the phenol degradation were investigated. The results indicated that Pd/CeO_x/Nano-G cathode would have promise for further practical application in organic wastewater treatment.

Keywords: Electrochemical Cathode; Nano-graphite; CeO_x; Pd Modification; Phenol Degradation

ARTICLE INFO

Received: 6 September 2021
Accepted: 20 October 2021
Available online: 26 October 2021

1. Introduction

Phenolic compounds, as a kind of ubiquitous, toxic, and harmful pollutants, have attracted extensive attention[1–3]. Advanced oxidation technology shows certain advantages over traditional microbial methods and physical adsorption methods in the treatment of phenolic pollutants, such as higher efficiency, more thorough reaction, and no secondary pollution[4,5]. Electrochemical advanced oxidation technology has been widely used because of its advantages of space-saving, easy operation, and high efficiency[6,7]. This technology mainly uses the generation of active species with strong oxidation ability and no selectivity during the electrochemical reaction, such as hydroxyl radical (•OH) and hydrogen peroxide (H_2O_2), to realize the degradation and mineralization of organic matter in water[8]. The electrochemical cell is mainly composed of an anode, cathode, and electrolyte, among which there are relatively many studies on anode materials[9,10]. In the electrochemical reaction process, the cathode mainly produces the reduction reaction of O_2 initiated by 2 electrons, and the generated H_2O_2 is further

decomposed into •OH under the action of catalyst, to realize the degradation reaction of organic matter catalyzed by cathode[10–12]. Therefore, researching and developing new efficient cathode materials great significantly improve the performance of the electrochemical cell.

In recent years, carbon materials (graphite, carbon black, activated carbon, etc.) are often used as a cathode to catalyze O_2 reduction reactions because of their cheap and stable characteristics[13–18]. Nano-graphite, as a new carbon nanomaterial, has excellent physical and chemical properties, for example, it has good thermal stability and conductivity. In particular, the porous structure and large specific surface area of Nano-graphite are conducive to the uniform and stable loading of other catalyst materials on its surface, to improve the catalytic performance of Nano-graphite[17,18]. Rare earth compounds have unique physical and chemical properties, so they are used in many fields. As an important rare earth element, cerium oxide (CeO_2) has been widely concerned because of its good performance as the catalyst, catalyst carrier, solid electrolyte in fuel cell, and oxygen sensing material[19,20]. In addition, noble metal materials such as Pd and Pt have an excellent catalytic effect on cathode oxygen reduction reaction, so they are often used to improve the performance of cathode materials[21,22]. The results of the author's previous work show that by regulating CeO_x (coexistence of Ce^{3+} and Ce^{4+}) to build a complex with Nano-graphite, we can not only promote the production of H_2O_2 but also convert it into •OH, to immensely improve the catalytic performance of the cathode[23]. On this basis, whether the electrocatalytic performance can be further improved by introducing precious metals remains to be studied.

In this work, ceria (CeO_x) and metal Pd co-modified Nano-graphite composite materials were prepared by chemical precipitation and formaldehyde reduction, then electrochemical cathode prepared by the hot pressing method for electrocatalytic degradation of phenol wastewater. SEM, XRD, and XPS were used to analyze the morphology and composition of the composites, optimize the reaction conditions and reveal the mechanism of improving its catalytic activity.

2. Experiment

2.1 Reagents and instruments

The main reagents used in the experiment are as follows: $Ce(NO_3)_3$•$6H_2O$(AR), $PdCl_2$(AR), natural flake graphite(200 mesh, 95% C), formaldehyde solution (AR), potassium permanganate (AR), absolute ethanol (AR), ammonia (AR), etc. SEM (Philips XL–30–ESEM–FEG), XRD(XRD–D/max III B), tube voltage 40 kV, tube current 30 mA, Cu Kα), XPS (PHI5700), voltage 12.5 kV, current 30 mA, Al Kα). The morphology, crystal structure, and element composition of a series of samples characterized. Analyzing the catalytic reaction products by ultraviolet-visible spectrophotometer (T6) and fluorescence spectrophotometer (LS55, Perkin Elmer).

2.2 Characterization method of material activity

2.2.1 Preparation of composite cathode

Use the stainless steel mesh after pickling and caustic washing as the electrode support. Place the beaker with composite materials in a constant temperature water bath pot at 65 ℃, and add an appropriate amount of binder polytetrafluoroethylene (PTFE) emulsion and dispersant anhydrous alcohol to the mixture under the stirring conditions. Put the mixed paste on the stainless steel net and roll it repeatedly with a roller press to make the paste firmly adhere to the stainless steel net. Place the composite electrode prepared above in distilled water, heat and boil for 30 min, take it out and dry it in an 80 ℃ oven for 2 h.

2.2.2 Electrochemical performance test method

The device consists of an electrolytic cell, DC regulated power supply (dual-channel DC power supply, DH1715A–5), diaphragm, anode and cathode electrodes, and air aeration device. The electrolytic cell is a plexiglass reactor with 120 mL. It uses cotton cloth as the diaphragm, self-made composite electrode as a cathode, titanium coated ruthenium

material as an anode, sodium sulfate as supporting electrolyte (0.1 M), simulating the degradation of phenol wastewater (100 mg/L) (the size of cathode and anode is 4 cm × 4 cm). The absorbance of phenol solution at different electrolysis times was measured with a T6 UV-Vis spectrophotometer at the wavelength of 510 nm. And then draw the phenol standard curve. Determine the concentration of phenol by 4-amino antipyrine spectrophotometry. The calculation formula is as follows: $X\% = (C_0 - C_t)/C_0 \times 100\%$, where C_0 is the initial concentration of phenol and C_t is the phenol concentration at time t.

Determination of H_2O_2 concentration: hydrogen peroxide is a strong oxidant and will be oxidized only reacting with a stronger oxidant. Therefore, potassium permanganate titration is used to detect the concentration of hydrogen peroxide. The reaction is as follows: $2KMnO_4 + 3H_2SO_4 + 5H_2O_2 \rightarrow K_2SO_4 + 2MnSO_4 + 5O_2\uparrow + 8H_2O$. The calculation formula of H_2O_2 concentration is as follows: $C = (V \times 34 \times 5 \times 0.002 \times 1000)/(25 \times 2)$, in which C is the concentration of H_2O_2; V is the volume of potassium permanganate.

Detection of hydroxyl radical: hightly fluorescent substances of 2-OHBZ and 3-OHBZ strong generate after the reaction of benzoic acid with hydroxyl radical, which can be indirectly determined by the change of fluorescence intensity. LS55 fluorescence spectrophotometer produced by Perkin Elmer company is used to detect the concentration of 3-OHBZ. The experimental conditions are as follows: the excitation wave is 305 nm, the emission wavelength is 300–600 nm, the incident and exit narrow are 10 nm, and the sensitivity is medium.

2.3 Experimental process

2.3.1 Preparation of Nano-graphite

Natural flake graphite with a particle size of 200 mesh is the raw material. Mix it with potassium permanganate, and pour them into a beaker filled with perchloric acid, then stirred evenly. Placed in a constant temperature water bath for 40 min. Transfer the mixture to a large container, and wash it repeatedly with distilled water until the filtrate is neutral, filter it and dry it in an 80 ℃ oven to obtain graphite interlayer compound. Put the graphite interlayer compound into a crucible and microwave expanded for 20 s to get expanded graphite. The prepared expanded graphite is added to ethanol solvent to form a uniform suspension, crushed in an ultrasonic cleaner for 12 h, and dried in an oven at 80 ℃ to obtain Nano-G.

2.3.2 Preparation of ceria

$Ce(NO_3)_3 \cdot 6H_2O$ was dissolved in deionized water to prepare $Ce(NO_3)_3$ solution with some concentration. Add a certain amount of ammonia to the above solution, stir with the magnetic force for 2 h, and then age. The precipitate was washed with deionized water and ethanol many times, dried in an 80 ℃ oven, and calcined in a muffle furnace at 450 ℃ for 2 h to obtain a light yellow ceria powder.

2.3.3 Preparation of ceria/Nano-graphite composites

CeO_{xn}/Nano-G composites were prepared by chemical precipitation method with Nano-graphite and cerium nitrate as raw materials. The specific process is as follows: $Ce(NO_3)_3 \cdot 6H_2O$ was dissolved in deionized water to prepare 100 mL of $Ce(NO_3)_3$ solution with some concentration. Add 1.5 g of Nano-graphite into the beaker containing the solution above, stir and mix evenly, add ammonia as precipitant, magnetic stirring for 12 h, and static aging at room temperature for 12 h. Wash the obtained precipitate with ethanol and deionized water many times, filter it, and then dry in an 80 degrees centigrade oven. After calcination at 450 degrees centigrade in a muffle furnace for 2 h, it obtains ceria/Nano-G, which was recorded as CeO_{xn}/Nano-G, and n was the mass percentage of $Ce(NO_3)_3 \cdot 6H_2O$ added (3.0%, 5.0%, 7.0%, 9.0%), which was successively marked as $CeO_{x3.0}$/Nano-G, $CeO_{x5.0}$/Nano-G, $CeO_{x7.0}$/Nano-G, $CeO_{x9.0}$/Nano-G.

2.3.4 Preparation of palladium and ceria co modified Nano-graphite composites

1.5 g $CeO_{x5.0}$/Nano-G composite was added to deionized water and stirred evenly at 80 ℃. Weigh an appropriate amount of palladium chloride ($PdCl_2$)

and dissolve it in concentrated hydrochloric acid. After palladium chloride is completely dissolved, add 15 mL of water for dilution, and then add it to the above solution drop by drop. Magnetic stirre at 80 ℃ for 2 h, cool to 40 ℃, add 36% formaldehyde solution drop by drop to the mixture above, stir for 30 min, then add 30% sodium hydroxide solution drop by drop, and adjust the pH of the mixture between 8–9. After repeated washing and filtration with deionized water then drying in an oven at 80 ℃, the obtained product is palladium/cerium oxide/Nano-graphite composite, which records as $Pd_m/CeO_{x5.0}$/Nano-G, *m* is the mass percentage of $PdCl_2$ added (1.0%, 2.5%, 3.0%), and then labeled as $Pd_{1.0}/CeO_{x5.0}$/Nano-G, $Pd_{2.0}/CeO_{x5.0}$/Nano-G, $Pd_{3.0}/CeO_{x5.0}$/Nano-G.

3. Results and discussion

3.1 Material composition and morphology analysis

As can be seen from **Figure 1(a)**, the XRD patterns of Nano-graphite show two diffraction peaks at 2θ = 26.6° and 54.6°, corresponding to the characteristic diffraction peaks of (002) and (004) crystal surfaces of graphite materials (JCPDS No. 08–0415)[24]. In CeO_x/Nano-G composite samples, new diffraction peaks appear at 2θ = 28.5°, 33.1°, 47.5°, and 56.4° respectively, corresponding to the characteristic diffraction peaks of (111), (200), (220) and (311) crystal planes of CeO_2, respectively. It indicates that cerium oxide has successfully loaded on the surface of Nano-graphite[25]. The diffraction peak at 2θ = 28.6° is sharp, which indicates that the loaded cerium oxide has a good crystallinity. The particle size of cerium oxide is about 10 nm calculated by the Scherer formula. In addition, the characteristic diffraction peak of graphite still exists in the composite sample, indicating that the crystal structure of graphite does not change significantly in the process of loading cerium oxide. In $Pd_{1.0}/CeO_{x5.0}$/Nano-G, it shows that 2θ = 40.1° is the characteristic diffraction peak of palladium (111) crystal plane (JCPDS No. 01–1201)[26], indicating that Palladium has successfully loaded on cerium oxide/Nano-graphite. Due to the low content of palladium, the intensity of the diffraction peak is weak.

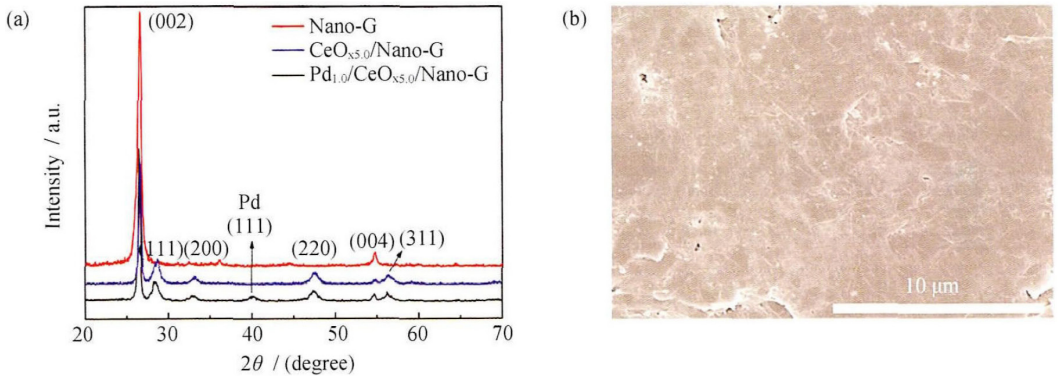

Figure 1. XRD patterns. **(a)** of Nano-G, $CeO_{x5.0}$/Nano-G and $Pd_{1.0}/CeO_{x5.0}$/Nano-G composite, and SEM image; **(b)** of $Pd_{1.0}/CeO_{x5.0}$/Nano-G composite cathode.

As illustrated in **Figure 1(b)**, the mixture of Pd/CeO_x/Nano-G, ethanol, and PTFE emulsion is more homogeneous. The addition of PTFE leads to uneven distribution of color on the electrode surface, and the white granular material on the electrode surface is palladium and cerium oxide particles loaded with CeO_x. In addition, the electrode surface is not smooth and dense but full of pits and gaps. The reason is that the loaded palladium and cerium oxide particles are filled between the Nano-graphite layers, forming a well conductive network on the electrode surface. The pores on the surface are conducive to the mass transfer of oxygen and increase the effective area of a three-phase reaction. It will be conducive to the occurrence of a cathode oxygen reduction reaction[22].

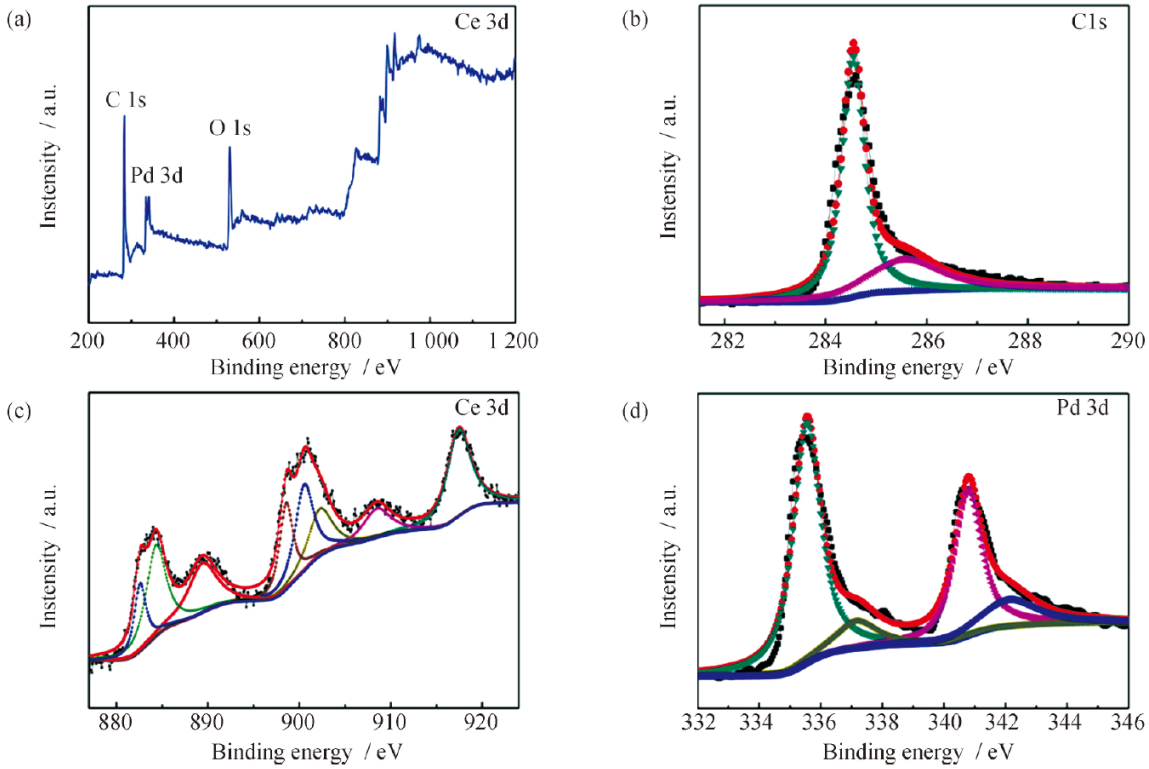

Figure 2. XPS spectrum of **(a)** $Pd_{1.0}/CeO_{x5.0}$/Nano-G composite, and **(b)** C 1s, **(c)** Ce 3d and **(d)** Pd 3d.

It shows that in **Figure 2(a)**, the $Pd_{1.0}/CeO_{x5.0}$/Nano-G composite contains the binding energy peaks of C ls, O 1s, Ce 3d, Ce 4p, and Pd 3d[27–30]. **Figure 2(b)** is the XPS spectrum of C 1s orbit. The characteristic peaks at the binding energies of 284.6 eV and 285.5 eV belong to the sp2 C–C bond and C–O single bond respectively[27,29]. According to the binding energy peak position of Ce 3d in **Figure 2(c)**, there are two valence states of Ce^{3+} and Ce^{4+} in the composite sample, of which the binding energy peaks at 884.3 eV and 902.2 eV belong to Ce^{3+}, 882.5 eV, 889.4 eV, 898.5 eV, 900.5 eV, 908.4 eV, while 917.4 eV belong to Ce^{4+}. So it infers that there are Ce_2O_3 and CeO_2 in the composite sample, and it is a mixed crystal phase[31,32]. **Figure 2(d)** is the XPS spectrum of Pd 3d, in which the peaks at 335.5 eV and 340.7 eV correspond to Pd^0 3d 5/2 and Pd^0 3d 3/2 respectively, indicating that palladium in the composite exists in the form of simple substance[26,28].

3. 2 Study on performance and mechanism of cathodic catalytic degradation of phenol

3.2.1 Performance of electrocatalytic degradation of phenol

It shows that in **Figure 3(a)**, under the condition of no air explosion, the degradation rate of phenol by Nano-G cathode is 70.3%. With the increase of the proportion of composite CeO_x, the activity of composite cathode gradually increases. The activity of the $CeO_{x5.0}$/Nano-G sample reaches 83.5%, and the activity decreases with the increase of the additional amount. The reason may be that the introduction of too much CeO_x will cover the active sites on the electrode surface. To prove the properties of the composites, it compared the degradation properties of Nano-G and $CeO_{x5.0}$/Nano-G electrodes under the condition of air explosion. The results showed that the degradation rate of phenol by $CeO_{x5.0}$/Nano-G electrode was 93.9%, which was significantly higher than that of the Nano-G electrode (79.2%). **Figure 3(b)** focuses on the effect of the introduction of PD on the performance of the $CeO_{x5.0}$/Nano-G cathode. The experimental results show that with the increase of Pd content, the performance of cathodic degradation of phenol is also improved. Under the same electrolysis conditions, after electrolysis for 80 min,

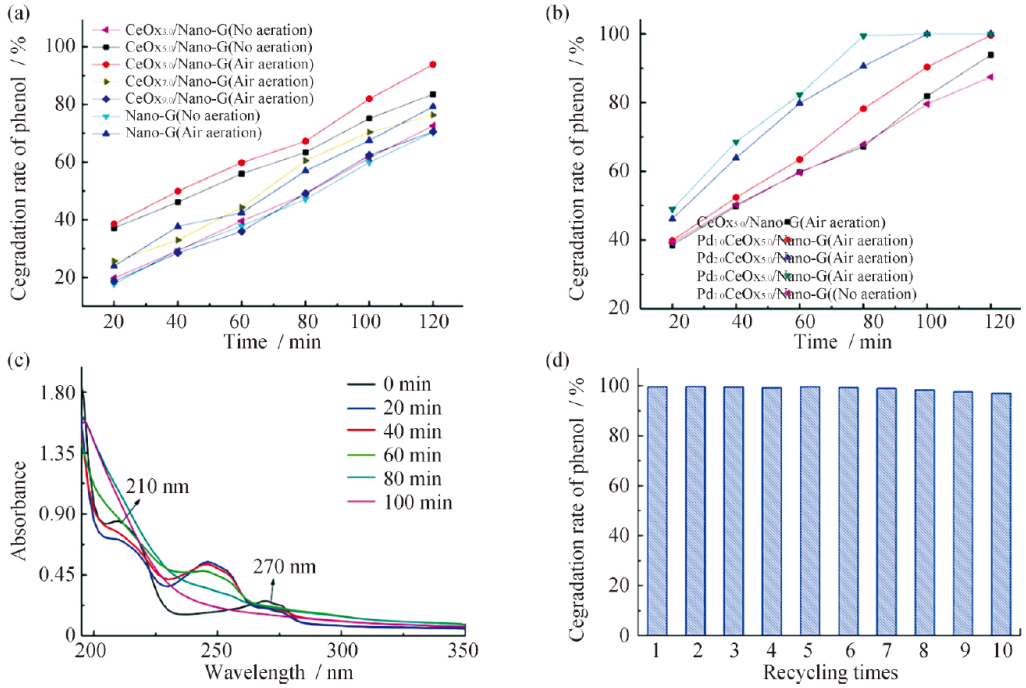

Figure 3. Electro-catalytic degradation of phenol by CeO_{xn}/Nano-G cathode with different CeO_x content **(a)**, Pdm/CeO_x/Nano-G cathode with different Pd content **(b)**, UV-Vis spectral scans of electrolyte on $Pd_{1.0}/CeO_{x5.0}$/Nano-G cathode at different electrolysis time **(c)**, and repeated utilization of $Pd_{1.0}/CeO_{x5.0}$/Nano-G cathode for electro-catalytic degradation of phenol **(d)**.

the corresponding phenol degradation rates of samples with palladium content of 0%, 1.0%, 2.0% and 3.0% were 67.2%, 78.2%, 90.6% and 99.5% respectively. After 120 min electrolysis, when the palladium content was 0% and 1.0%, the phenol degradation rates in the cathode chamber were 93.9% and 99.6% respectively. It shows that palladium plays an important role in the catalytic degradation of phenol. However, since palladium is the first platinum group precious metal, from the perspective of cost, this paper focuses on the mechanism of $Pd_{1.0}/CeO_{x5.0}$/Nano-G composites. The UV-Vis absorption spectra of phenol solution were studied under the conditions of different degradation reaction times. It shows that in **Figure 3(c)**, the initial phenol solution has a strong absorption peak at 210 nm and 270 nm, which is the characteristic absorption peak of phenol. With the gradual progress of the electrolytic reaction, phenol oxidized, the characteristic structure destroyed, and the absorption peak gradually weakens and finally disappears. The degradation of phenol includes three stages: (1) the conjugated system of double bond structure of phenol is opened to form benzoquinone and other substances. (2) benzoquinone is converted into some small molecular carboxylic acids. (3) it is oxidized to carbon dioxide and water. After electrolysis for 20 min, it can see the absorption peak of benzoquinone at 245 nm. With the passage of degradation time, the absorption peak of benzoquinone gradually weakens and finally disappears, indicating that phenol in the system has been degraded[18]. In addition, it further investigated the cyclic stability of the samples. It shows that in **Figure 3(d)**, the degradation rate of phenol in the cathode chamber does not decrease significantly after reusing the palladium/cerium oxide/Nano-graphite composite cathode 10 times. If it is continuously used, the degradation rate of phenol begins to decline, but still maintains a high degradation rate of phenol. After 15 times of reuse, it can reach 90%, and the electrode does not fall off or bubble during use. It shows that the electrode has good stability and can be reused. It has broad prospects in the electrocatalytic treatment of organic wastewater[33].

3.2.2 Mechanism analysis of activity enhancement

To reveal the reason for the high cathode ac-

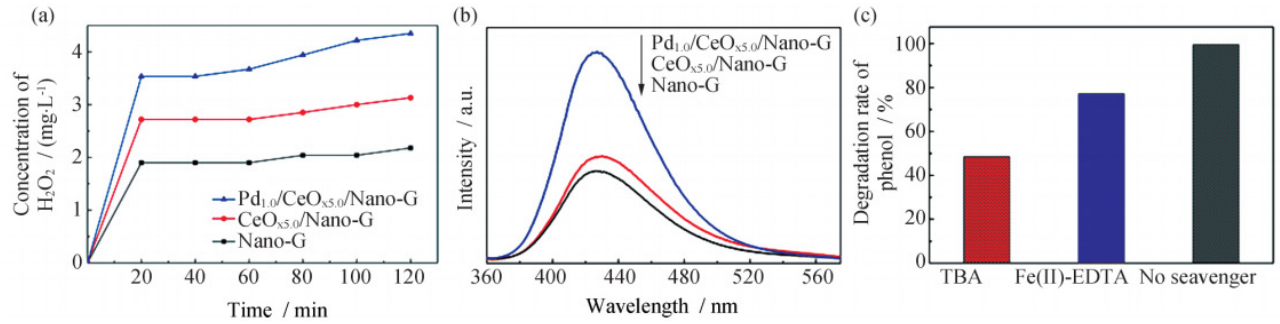

Figure 4. Concentration of H_2O_2 **(a)** and FL spectra **(b)** by Nano-G, $CeO_{x5.0}$/Nano-G and $Pd_{1.0}/CeO_{x5.0}$/Nano-G cathodes; degradation of phenol with or without different scavengers by $Pd_{1.0}/CeO_{x5.0}$/Nano-G cathode **(c)** (Wastewater pH: 7, current density: 39 mA/cm^{-2}, phenol: 100 mg/L and electrolysis time: 120 min; aeration.

tivity of $Pd_{1.0}/CeO_{x5.0}$/Nano-G, the concentration of H_2O_2 produced in the reaction process was analyzed. As shown in **Figure 4(a)**, it compared the H_2O_2 concentrations in Nano-G, $CeO_{x5.0}$/Nano-G and $Pd_{1.0}/CeO_{x5.0}$/Nano-G cathode chambers, and analyzed after 120 min of reaction. The results show that the concentration of H_2O_2 basically reaches saturation within the first 20 min of the electrolytic reaction, and the concentration of hydrogen peroxide does not increase significantly with the increase of time. It is mainly due to the high concentration of dissolved oxygen in the cathode chamber at the initial stage of electrolysis. More hydrogen peroxide is produced by reduction[34]. With the increase of electrolysis time, the cathode is gradually alkaline, while hydrogen peroxide is unstable under alkaline conditions and is easy to convert or decompose into peroxy hydroxyl anion. On the other hand, the temperature of the electrolyte increases with the increase of electrolytic time, and the content of dissolved oxygen in the solution decreases with temperature increasing, which reduces the reduction reaction of cathode oxygen molecules. At high temperatures, H_2O_2 is unstable and easily converted to •OH. Therefore, the concentration of hydrogen peroxide does not increase significantly with the increase of time. The concentration of hydrogen peroxide produced by $Pd_{0.1}CeO_x$/Nano-G cathode was significantly higher than that of CeO_x/Nano-G cathode (3.13 mg/L) and Nano-G cathode (2.18 mg/L) when the reaction time was 120 min. The above results indicate that the co-modification of cerium oxide and Pd can effectively promote the reduction reaction process of cathode O_2, thus showing a higher generation capacity of hydrogen peroxide[23].

Figure 4(b) shows the hydroxyl radical capture fluorescence spectra of Nano-G, CeO_x/Nano-G, $Pd_{1.0}/CeO_x$/Nano-G cathodes after electrolysis for 120 min. It shows that in **Figure 4(b)**, the characteristic absorption peak of 3-OHBZ appears at 415 nm, which indicates that hydroxyl radical generates in the electrolysis process, and the fluorescent substance 3-OHBZ generates after interaction with benzoic acid[35]. After electrolysis for 120 min, the fluorescence intensity of CeO_x/Nano-G composite cathode was higher than that of Nano-G cathode, indicating that the hydroxyl radical produced by CeO_x/Nano-G composite cathode was more than that of Nano-G cathode. The fluorescence intensity of $Pd_{1.0}/CeO_x$/Nano-G composite cathode is higher than that of CeO_x/Nano-G composite cathode, indicating that Pd/CeO_x/Nano-G composite cathode produces the most hydroxyl radicals. The fluorescence detection of hydroxyl radical shows that the supported palladium can better catalyze the formation of H_2O_2 and the generation of free radicals. This is because palladium has better electron reduction catalytic ability and can also catalyze the decomposition of hydrogen peroxide into hydroxyl radical.

In order to determine the active oxidation species that play an important role in the cathodic electrocatalytic degradation of phenol, different active radical capture agents were added in the electrocatalytic degradation of phenol. Under the same

electrolytic conditions, the effects of different radical capture agents on the degradation effect of phenol were investigated to determine the oxidation effect of different active radicals on Phenol in the electrolytic process[36,37]. Prepare a 1 mol/L solution of hydroxyl (•OH) capture agent tert butyl alcohol (TBA) and hydrogen peroxide capture agent Fe^{2+}-EDTA. Add 10 mL to 100 mL phenol electrolyte with a concentration of 100 mg/L respectively. After electrolysis for 120 min, the phenol degradation rate in the cathode chamber is shown in **Figure 4(c)**. The addition of different active radical capture agents had a certain effect on the degradation of phenol. Among them, the addition of hydroxyl radical capture agent TBA had an obvious effect on the degradation rate of phenol, and the degradation rate of phenol decreased by 51%. The addition of hydrogen peroxide capture agent Fe^{2+}-EDTA had little effect on the degradation rate of phenol, and the degradation rate of phenol decreased by only 22.3%. This shows that •OH is the main active species of an oxidation reaction in the process of electrocatalytic degradation of phenol. At the same time, the supported palladium can catalyze the cathode oxygen reduction, adsorb oxygen molecules through its d orbital hole, break its O–O bond, react with H^+ in the solution, promote the generation of hydrogen peroxide and hydroxyl radical, and improve the degradation rate of phenol in the cathode chamber[38].

4. Conclusion

In this paper, Nano-G composites co-modified by elemental Pd and miscible CeO_x successfully prepared by simple chemical precipitation method and formaldehyde reduction method and were used to study the performance of cathodic electrocatalytic degradation of phenol. Compared with pure Nano-G and $CeO_{x0.5}$/Nano-G, $Pd_{1.0}/CeO_{x0.5}$/Nano-G samples show higher activity with and without air explosion, which is mainly due to Ce^{3+} and Ce^{4+} valence states of CeO_x in the complex, which is conducive to initiating O_2 reduction reaction to produce H_2O_2, and co-catalyzing with elemental Pd to produce more active species •OH. Thus, the complex showed higher performance of electrocatalytic degradation of phenol.

Conflict of interest

The authors declare that they have no conflict of interest.

Acknowledgements

National Natural Funds–Guangdong Joint Fund Project (U1401245); Basic Research Funds of Heilongjiang Provincial Universities (RCCXYJ201803); Science and Technology Research and Development Project of Heilongjiang Provincial Higher Education Department (TSTAU–R2018022).

References

1. Vaiano V, Matarangolo M, Murcia JJ, *et al.* Enhanced photocatalytic removal of phenol from aqueous solutions using ZnO modified with Ag. Applied Catalysis B: Environmental 2018; 225: 197–206.
2. Chen Y, Yan J, Ouyang D, *et al.* Heterogeneously catalyzed persulfate by CuMgFe layered double oxide for the degradation of phenol. Applied Catalysis A: General 2017; 538: 19–26.
3. Berenguer R, Sieben JM, Quijada C, *et al.* Electrocatalytic degradation of phenol on Pt-and Ru-doped Ti/SnO_2-Sb anodes in an alkaline medium. Applied Catalysis B: Environmental 2016; 199: 394–404.
4. Ooi YK, Yuliati L, Lee SL. Phenol photocatalytic degradation over mesoporous TUD-1-supported chromium oxide-doped titania photocatalyst. Chinese Journal of Catalysis 2016; 37(11): 1871–1881.
5. Moreira FC, Boaventura RAR, Brillas E, *et al.* Electrochemical advanced oxidation processes: A review on their application to synthetic and real wastewaters. Applied Catalysis B: Environmental 2017; 202: 217–261.
6. Li D, Guo X, Song H, *et al.* Preparation of RuO_2-TiO_2/Nano-graphite composite anode for electrochemical degradation of ceftriaxone sodium. Journal of Hazardous Materials 2018; 351: 250–259.
7. Duan X, Xu F, Wang Y, *et al.* Fabrication of a hydrophobic SDBS-PbO_2 anode for electrochemical degra-

dation of nitrobenzene in aqueous solution. Electrochimica Acta 2018; 282: 662–671.
8. Boye B, Dieng MM, Brillas E. Degradation of Herbicide 4-Chlorophenoxyacetic acid by advanced electrochemical oxidation methods. Environmental Science & Technolgy 2002; 36(13): 3030–3035.
9. Feng Y, Yang L, Liu J, *et al.* Electrochemical technologies for wastewater treatment and resource reclamation. Environmental Science: Water Research & Technology 2016; 2(5): 800–831.
10. Xu D, Song X, Qi W, *et al.* Degradation mechanism, kinetics, and toxicity investigation of 4-bromophenol by electrochemical reduction and oxidation with Pd-Fe/graphene catalytic cathodes. Chemical Engineering Journal 2018; 333: 477–485.
11. Song X, Shi Q, Wang H, *et al.* Preparation of Pd-Fe/graphene catalysts by photocatalytic reduction with enhanced electrochemical oxidation-reduction properties for chlorophenols. Applied Catalysis B: Environmental 2017; 203: 442–451.
12. Wang H, Sun D, Bian Z. Degradation mechanism of diethyl phthalate with electrogenerated hydroxyl radical on a Pd/C gasdiffusion electrode. Journal of Hazardous Materials 2010; 180(1-3): 710–715.
13. Liu S, Zhao X, Sun H, *et al.* The degradation of tetracycline in a photo-electro-Fenton system. Chemical Engineering Journal 2013; 231: 441–448.
14. Bocos E, Alfaya E, Iglesias O, *et al.* Application of a new sandwich of granular activated and fiber carbon as cathode in the electrochemical advanced oxidation treatment of pharmaceutical effluents. Separation and Purification Technology 2015; 151: 243–250.
15. Paz EC, Aveiro LR, Pinheiro VS, *et al.* Evaluation of H_2O_2 electrogeneration and decolorization of orange II azo dye using tungsten oxide nanoparticle-modified carbon. Applied Catalysis B: Environmental 2018; 232: 436–445.
16. Hu X, Zhang H, Sun Z. Adsorption of low concentration ceftazidime from aqueous solutions using impregnated activated carbon promoted by iron, copper and aluminum. Applied Surface Science 2017; 392: 332–341.
17. Yu X, Qiang L. Preparation for graphite materials and study on electrochemical degradation of phenol by graphite cathodes. Advances in Materials Physics and Chemistry 2012; 2(2): 63–68.
18. Yu X, Sun T, Wan J. Preparation for Mn/Nanographite materials and study on electrochemical degradation of phenol by Mn/Nanographite cathodes. Journal of Nanoscience and Nanotechnology 2014; 14(9): 6835–6840.
19. Baby TT, Rakhi RB, Ravi N, *et al.* Cerium oxide dispersed multi walled carbon nanotubes as cathode material for flexible field emitters. Journal of Nanoscience and Nanotechnology 2012; 12: 6718–6723.
20. Rangel R, López-Mercado J, Bartolo P, *et al.* Nanostructured-[CeO_2, La_2O_3, C]/TiO_2 catalysts for lignin photodegradation. Science of Advanced Materials 2012; 4(5): 573–578.
21. Wang H, Wang J. Comparative study on electrochemical degradation of 2,4-dichlorophenol by different Pd/C gas-diffusion cathodes. Applied Catalysis B: Environmental 2009; 89(1-2): 111–117.
22. Li D, Sun T, Wang L, *et al.* Enhanced electro-catalytic generation of hydrogen peroxide and hydroxyl radical for degradation of phenol wastewater using MnO_2/Nano-G|Foam-Ni/Pd composite cathode. Electrochimica Acta 2018; 282: 416–426.
23. Yu L, Yu X, Sun T, *et al.* Preparation for CeO_2/Nanographite composite materials and electrochemical degradation of phenol by CeO_2/Nanographite cathodes. Journal of Nanoscience and Nanotechnology 2015; 15(7): 4920–4925.
24. Jia J, Li D, Wan J, *et al.* Characterization and mechanism analysis of graphite/C-doped TiO_2 composite for enhanced photocatalytic performance. Journal of Industrial and Engineering Chemistry 2016; 33: 162–169.
25. Seong G, Dejhosseini M, Adschiri T. A kinetic study of catalytic hydrothermal reactions of acetaldehyde with cubic CeO_2 nanoparticles. Applied Catalysis A: General 2018; 550: 284–296.
26. Zhang M, Ning T, Zhang S, *et al.* Response time and mechanism of Pd modified TiO_2 gas sensor. Materials Science in Semiconductor Processing 2014; 17: 149–154.
27. Jia J, Li D, Cheng X, *et al.* Construction of graphite/TiO_2/nickel foam photoelectrode and its enhanced photocatalytic activity. Applied Catalysis A: General 2016; 525: 128–136.

28. Li D, Jia J, Zheng T, *et al.* Construction and characterization of visible light active Pd nano-crystallite decorated and C-N-S-codoped TiO_2 nanosheet array photoelectrode for enhanced photocatalytic degradation of acetylsalicylic acid. Applied Catalysis B: Environmental 2016; 188: 259–271.
29. Li D, Xing Z, Yu X, *et al.* One-step hydrothermal synthesis of C-N-S-tridoped TiO_2-based nanosheets photoelectrode for enhanced photoelectrocatalytic performance and mechanism. Electrochimica Acta 2015; 170: 182–190.
30. Fiala R, Vaclavu M, Rednyk A, *et al.* Pt-CeO_x thin film catalysts for PEMFC. Catalysis Today 2015; 240: 236–241.
31. Lee SM, Hong SC. Promotional effect of vanadium on the selective catalytic oxidation of NH_3 to N_2 over Ce/V/TiO_2. Applied Catalysis B: Environmental 2015; 163: 30–39.
32. Larachi F, Pierre J, Adnot A, *et al.* Ce 3d XPS study of composite $Ce_xMn_{1-x}O_{2-y}$ wet oxidation catalysts. Applied Surface Science 2002; 195: 236–250.
33. Yu L. Preparation of ceria nano graphite composite cathode and its degradation of phenol (in Chinese) [Master's thesis]. Harbin, Heilongjiang University; 2014.
34. Wang W, Yu J, Zou J, *et al.* Mechanism for enhancing biodegradability of antibiotic pharmacy wastewater by in-situ generation of H_2O_2 and radicals over MnO_x/nano-G/2-EAQ/AC cathode. Electrochimica Acta 2016; 191: 426–434.
35. Song YY, Roy P, Paramasivam I, *et al.* Voltage-induced payload release and wettability control on TiO_2 and TiO_2 nanotubes. Angewandte Chemie International Edition 2010; 49(2): 351–354.
36. Li F, Wang X, Zhao Y, *et al.* Ionic-liquid-assisted synthesis of high-visible-light-activated N-B-F-tri-doped mesoporous TiO_2 via a microwave route. Applied Catalysis B: Environmental 2014; 144: 442–453.
37. Chen Y, Lu A, Li Y, *et al.* Naturally occurring sphalerite as a novel cost-effective photocatalyst for bacterial disinfection under visible light. Environmental Science & Technology 2011; 45(13): 5689–5695.
38. Wang H, Bian Z, Lu G, *et al.* Preparation of multifunctional gas-diffusion electrode and its application to the degrading of chlorinated phenols by electrochemical reducing and oxidizing processes. Applied Catalysis B: Environmental 2012; 125: 449–456.